



Brussel, 25 June 2013

Dr. Bernard Delhousse
BELSPO
Louizalaan 231
1050
Brussel

Subject: Final report for the post-doctoral research of Dr. Sunil ADAVANAL PETER

Dear Dr. Delhousse,

Please find the attached final report of Dr. Sunil ADAVANAL PETER regarding his post-doctoral research from 01 January, 2012 to 30 April, 2013 under the framework of “International S & T Cooperation: Post-Doc Fellowships To Non-EU Researchers”. During his tenure, Dr. Adavanal has studied the separation of CO₂ and CH₄ in metal organic framework (MOF) adsorbent, amino-MIL-53(Al). A great achievement was the design and construction of an experimental setup to study the behavior of flexible Metal Organic Frameworks in Pressure Swing Adsorption (PSA). He also developed a PSA process using a single adsorbent column experimental setup. His experiments lead to the understanding of the separation mechanism with mixtures, which is of great importance with respect to the development of industrial processes.

He has presented his research work in an international conference and also has an accepted manuscript in a reputed journal to his credit. One more manuscript from this research is being prepared for submission in a reputed journal. The exposure to sophisticated adsorption setups and other analytical instruments has increased his expertise in the field of adsorptive separation of gases, which will enable him to secure a scientist or faculty job in his home country. For our lab, this project was an important added value, since he introduced new know-how in our group. The PSA setup build in the frame of this project could be used for any future gas separation studies in the department. It could be also possible to have further collaboration to jointly publish the research works in future.

Yours sincerely,

Joeri Denayer

**Kinetic Gas Separation using Small Pore Metal Organic Frameworks:
Dynamic Desorption and Pressure Swing Adsorption Studies of CO₂ and CH₄
in Amino-MIL – 53 (Al) for Biogas Upgradation**

Final report of the BELSPO sponsored research project co-funded by Marie Curie

Actions of the European Commission

Submitted by

Dr. Sunil Adavanal Peter

Under the supervision of

Prof. Dr. Joeri F. M. Denayer

Prof. Dr. Gino V. Baron

Department of Chemical Engineering (CHIS)

Vrije Universiteit Brussel

Pleinlaan 2, 1050 Brussels

Belgium

Table of Contents

1. Introduction	1
2. Objectives	1
3. Experimental	2
4. Results as discussion	4
5. Conclusions	13
Reference	14
List of publications	15

1. Introduction

Global warming due to increased concentrations of greenhouse gases in the atmosphere is of great concern as it is linked to unwanted climate changes [1, 2]. Carbon dioxide, methane, nitrous oxide, fluorocarbons, etc., are the major components of greenhouse gases. Even though the amount of CO₂ present in the atmosphere is greater than CH₄, the global warming potential of CH₄ is 21 times higher than that of CO₂ and therefore, the emission of CH₄ to atmosphere must be reduced [3, 4]. The major source of CH₄ to atmosphere is biogas, which is composed of around 55 - 70% CH₄, 30 - 40 % CO₂ and smaller amounts of NH₃, H₂S, N₂ and hydrocarbons depending on the source of production. Biogas is an alternative source of renewable energy, but its heating value is very low compared to natural gas due to significant amount of CO₂ present in it. To increase the energy content and also to avoid the pipeline and equipment corrosion, the CO₂ content for pipeline grade biomethane should be less than 2 – 3% [5]. Water scrubbing, amine absorption, membrane separation and adsorption process are the technologies used for the removal of CO₂ to upgrade the biogas [6].

Adsorption, especially pressure swing adsorption (PSA) or vacuum swing adsorption (VSA) process, is a commercially established process for the separation of gas mixtures in chemical industry. The selection of a suitable adsorbent for a particular system is the biggest challenge in the adsorption process. Presently, zeolites and porous carbon materials are the adsorbents mainly used for the separation of gaseous systems like N₂/O₂, CH₄/N₂, O₂/N₂, and olefin/paraffin [7]; new adsorbents are still needed to optimize these separation processes to make them commercially more attractive. Metal–organic frameworks (MOFs) have emerged as a new type of functional materials as adsorbents for the separation of various gaseous and liquid systems, and have witnessed explosive development and rapid progress over the past two decades [8]. Amino-MIL-53(Al) is an example of a MOF with flexible framework structure, with interesting features for the separation of CO₂ from gas mixtures [9]. When the pores of this MOF are in the contracted state, they exclude CH₄ of being adsorbed, which results in a very large selectivity in the separation of CO₂ from CH₄. In the present work, we studied the dynamic desorption of CO₂ from amino-MIL-53(Al) adsorbent. Breakthrough desorption experiments were performed with the adsorbent pre-saturated with a typical biogas composition [10] of 40% CO₂ – 60% CH₄ feed mixture at different temperatures and pressures. We also studied pressure swing adsorption for the separation of CO₂ – CH₄ gas mixture using amino-MIL-53, and compare the results with the well-known adsorbent, 13X zeolite.

2. Objectives

The objectives of this project were as follows;

- i) To study the dynamic desorption of CO₂ in amino-MIL-53 (Al) as it plays an important role in the design of pressure swing adsorption (PSA) process for the upgradation of biogas.
- ii) To study the size exclusion mechanism of CH₄ in amino-MIL-53(Al) at different pressures.
- iii) Compare the amino-MIL-53(Al) adsorbent with 13X zeolite in breakthrough and PSA measurements.

3. Experimental

3.1 Materials

Amino-MIL-53(Al), synthesized at Delft University of Technology [11], and 13X zeolite (Si/Al = 1.23) granules (500 μm) supplied by UOP were used as adsorbents. CO_2 (99.995%), CH_4 (99.95%), and He (99.995%) supplied by Air Liquide were used for the adsorption isotherm measurements as well as the breakthrough measurements.

3.2 Adsorption isotherm measurements

Adsorption isotherms were measured in a magnetic suspension gravimetric adsorption setup (Rubotherm GmbH) at 303, 318, and 333K and up to 40 bar. Prior to the adsorption measurement, around 200 mg of the adsorbent samples was activated under vacuum at a heating rate of 1 K/min up to 473 K and 623 K respectively for amino-MIL-53(Al) and 13X and kept at that temperature for around 8 h before cooling down to the adsorption temperature. The isotherm temperatures of the samples were controlled using a Julabo thermostat.

3.3 Adsorption-desorption breakthrough measurements

Adsorption-desorption breakthrough measurements were carried out in an in-house built breakthrough set up with a column length of 100 mm and internal diameter of 4.56 mm for both amino-MIL-53(Al) and 13X. Amino-MIL-53(Al) powder was made in to pellets (500-630 μm) before doing the breakthrough experiment and was activated *in situ* under helium flow at a heating rate of 5 K/min up to 473 K and kept at that temperature for 4 h before cooling down to the breakthrough experiment temperature. 13 X granules (500 μm) were heated up to 623 K at a heating rate of 5 K/min under helium flow and kept at that temperature for 6 h before cooling down to adsorption temperature. Around 715 mg of amino-MIL-53(Al) and 972 mg of 13 X were used for the breakthrough experiments. Adsorption-desorption breakthrough experiments were carried out at 1, 5, and 30 bar for amino-MIL-53(Al) and, at 1 and 5 bar for 13 X. 40% CO_2 and 60% CH_4 at a total flow of 20 Nml/min was used as the feed mixture for all the adsorption breakthrough measurements and 20 Nml/min of He purge was used for the dynamic desorption measurements. For the breakthrough measurements at 1 bar, the adsorbent column outlet was directly open to the atmosphere and a portion of the outlet flow was passed through an online mass spectrometer (MS) to monitor the outlet concentration. The outlet flow was diluted with nitrogen flow before connecting to the MS, in order to get a linear response of the outlet flow. For the breakthrough measurements at high pressures (5 and 30 bar), the outlet of the adsorbent column was connected to a backpressure regulator to maintain the particular adsorption pressures inside the column. A mass flow meter was also connected before the back pressure regulator to measure the exact outlet flow rate from the column and a small portion of this outlet flow was connected through a 50 μ capillary to the online MS to measure the outlet concentration. From the outlet concentration and outlet flow rate, the flow rates of individual components were calculated. The adsorption and desorption breakthrough measurements were carried out at 303, 318, and 333 K and in some cases, the desorption was carried out by increasing the column temperature at a rate of 5 K/min up to 473 K under He flow to desorb the adsorbed molecules easily.

The amount adsorbed of component a , q_a was calculated as:

$$q_a = \frac{(F\tau_a - \varepsilon VP/RT)y_a}{m_{ads}}$$

where F is the total flow rate (mmol/min); τ_a is the mean residence time (min); ε is the total adsorbent column porosity; V is volume of the column (ml); m_{ads} is the mass of the adsorbent (g); P is the total pressure inside the column (bar); y_a is the mole fraction of component a ; R is the ideal gas constant (8.31×10^{-2} ml bar K⁻¹ mmol⁻¹); and T is the column temperature (K). The mean residence time for adsorption breakthrough was calculated as:

$$\tau_a = \int_0^{t_\infty} \left(1 - \frac{F_a}{F_{ao}}\right) dt$$

where F_a is the outlet flow rate of component a ; and F_{ao} is the feed flow rate of component a . The mean residence time for the desorption breakthrough curve was calculated as:

$$\tau_a = \int_0^{t_\infty} \left(\frac{F_a}{F_{ao}}\right) dt$$

The mean residence time was corrected for the dead volume caused by the tubing and fittings of the breakthrough setup. Both pure component selectivity (calculated from the pure component isotherms) as well as dynamic binary adsorption selectivity (from breakthrough measurements) $\alpha_{a/b}$, of component a over component b were calculated as:

$$\alpha_{a/b} = \frac{q_a/y_a}{q_b/y_b}$$

where q_a and q_b are amount of components a and b adsorbed, and y_a and y_b are the mole fractions of components a and b at particular feed pressure.

3.4 Pressure swing adsorption (PSA) measurements

Pressure swing adsorption (PSA) studies were carried out in an in-house built single column PSA setup as shown in Fig.1. This experimental unit was built in the frame of this project. The same adsorbent columns used for breakthrough measurements were used for PSA measurements also. Two of types of PSA cycle configurations were used in this study. The First one was a normal Skarstrom cycle contains i) Pressurization with feed, ii) Adsorption, iii) Blowdown, and iv) Purging with product at atmospheric pressure to regenerate the column for consecutive cycles. In the second configuration, the regeneration of column was carried out by evacuation at low pressure using a vacuum pump and the cycle steps were i) Pressurization with feed, ii) Adsorption, iii) Evacuation, and iv) Pressurization with product (in some measurements, only feed pressurization was used). This process can be called as pressure vacuum swing adsorption (PVSA) process. Both amino-MIL-53(Al) and 13X zeolite adsorbent columns were activated initially as mentioned above and filled with CH₄ before starting the PSA measurements. The cycle steps were repeated until the process attained cyclic steady state (CSS). The product concentration was

measured using a mass spectrometer (MS). The process performance parameters such as purity, recovery and productivity were calculated as follows:

$$\text{Purity} = \frac{\int_0^{t_{\text{ads}}} F_{\text{raff}} \cdot y_{\text{CH}_4} dt}{\int_0^{t_{\text{ads}}} F_{\text{raff}} dt}$$

where t_{ads} is the adsorption step time; F_{raff} is the raffinate flow rate; y_{CH_4} is CH_4 mole fraction in the raffinate stream.

$$\text{Recovery} = \frac{\text{Amount CH}_4 \text{ in the product} - \text{Amount of CH}_4 \text{ used for purge}}{\text{Amount CH}_4 \text{ in the feed}}$$

$$\text{Productivity} = \frac{\text{Amount CH}_4 \text{ in the feed} \times \text{Recovery}}{\text{Cycle time} \times \text{weight of adsorbent}}$$

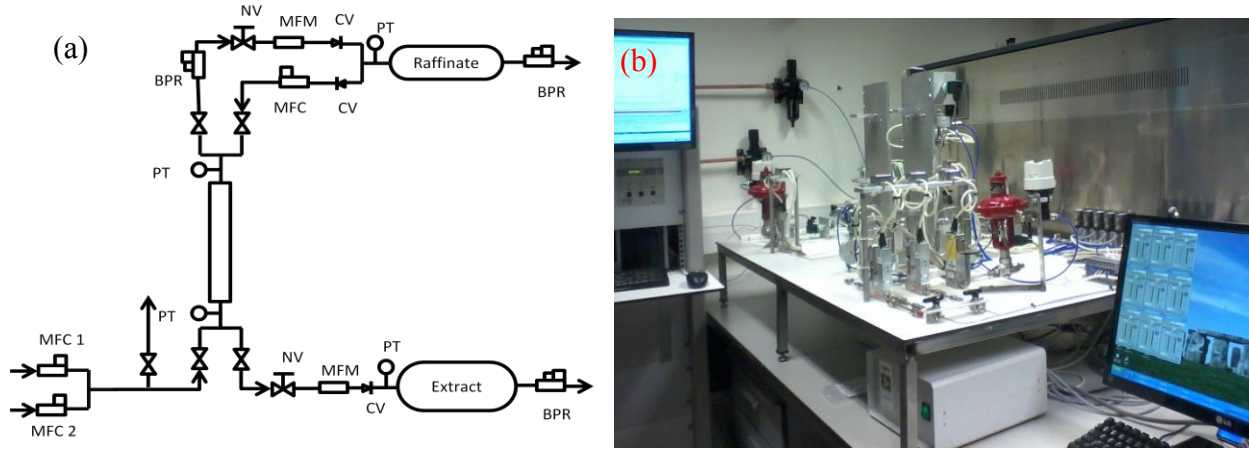


Fig. 1 (a) Schematic diagram and (b) photograph of a single column PSA setup.

4. Results and discussion

4.1 Adsorption isotherms

The adsorption and desorption isotherms of CO_2 and CH_4 in amino-MIL-53(Al) were measured at different temperatures up to 40 bar pressure as shown in Fig. 2. The CO_2 adsorption capacity at 303 K reached a plateau initially around 5 bar and again increased around 10 bar pressure and reached a second plateau around 40 bar. The desorption isotherm branch at 303K showed a large hysteresis and met back the adsorption isotherm around 3 bar. At 318 and 333K, the CO_2 adsorption capacity from the first adsorption plateau started to increase around 20 bar and requires much higher pressure than 40 bar to reach the second plateau. For CH_4 , there was negligible adsorption initially and the adsorption capacity started to increase when the pressure was greater than 1 bar. CH_4 isotherm also showed hysteresis during desorption. Amino-MIL-53(Al) is a flexible MOF with distinct crystallographic structures at room temperature. Recent *in situ* XRD measurements showed that amino-MIL-53(Al) adopts a very narrow

pore form (*vnp*) at low pressure; guest molecule adsorption at low pressure transforms this structure to the *np* form [11]. At much higher pressure, a transition from *np* to *lp* occurs. This very narrow pore form is responsible for the exclusion of CH₄ at <1 bar pressure, which might be exploited for kinetic separations, as discussed below.

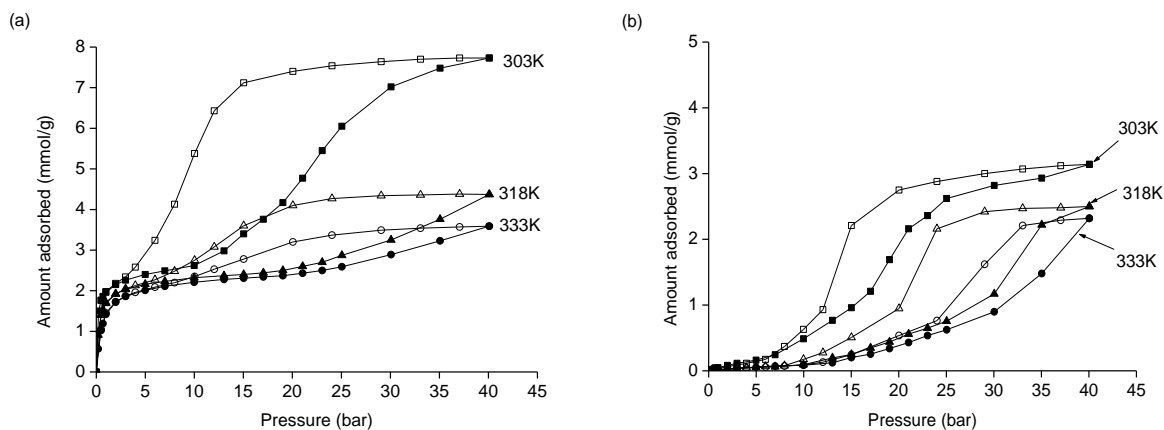


Fig. 2 Adsorption and desorption isotherms of (a) CO₂ and (b) CH₄ in amino-MIL-53(Al) at different temperatures (closed symbol for adsorption and open symbol for desorption).

The adsorption and desorption isotherms of CO₂ and CH₄ in 13X zeolite at different temperatures and pressure up to 40 bar are shown in Fig. 3. The CO₂ adsorption reached a plateau around 10 bar, but CH₄ adsorption kept on increasing till 40 bar. The initial uptake of CO₂ in 13X was very steep at low pressure compared to CH₄ adsorption. Desorption of CO₂ from 13X was completely reversible with a very small hysteresis, while the CH₄ desorption was completely reversible without any hysteresis. The strong electrostatic interaction of CO₂ with extra-framework Na⁺ present inside the cavity of 13X may cause this hysteresis, while the electrostatic interaction of CH₄ with Na⁺ is weak compared to the interaction of CO₂ with Na⁺ ion [12].

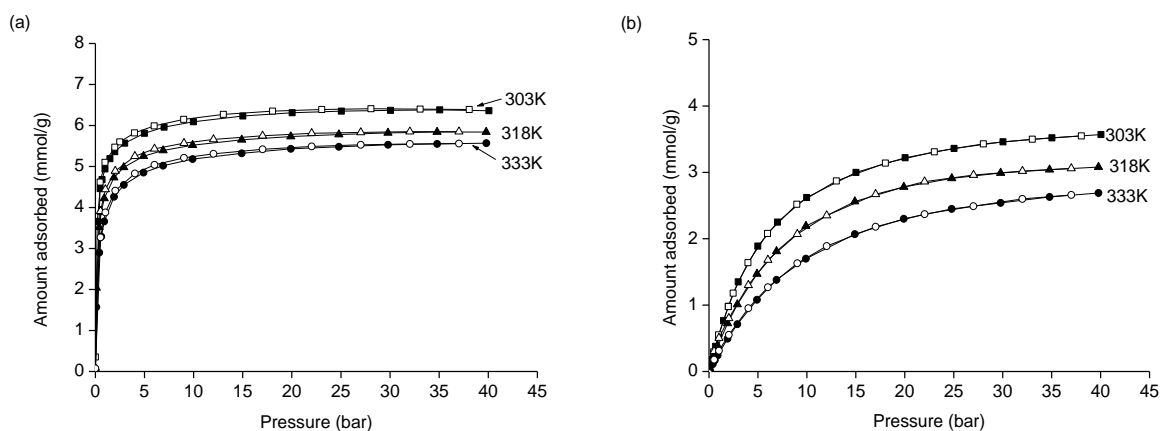


Fig. 3 Adsorption and desorption isotherms of (a) CO₂ and (b) CH₄ in 13X zeolite at different temperatures (closed symbol for adsorption and open symbol for desorption).

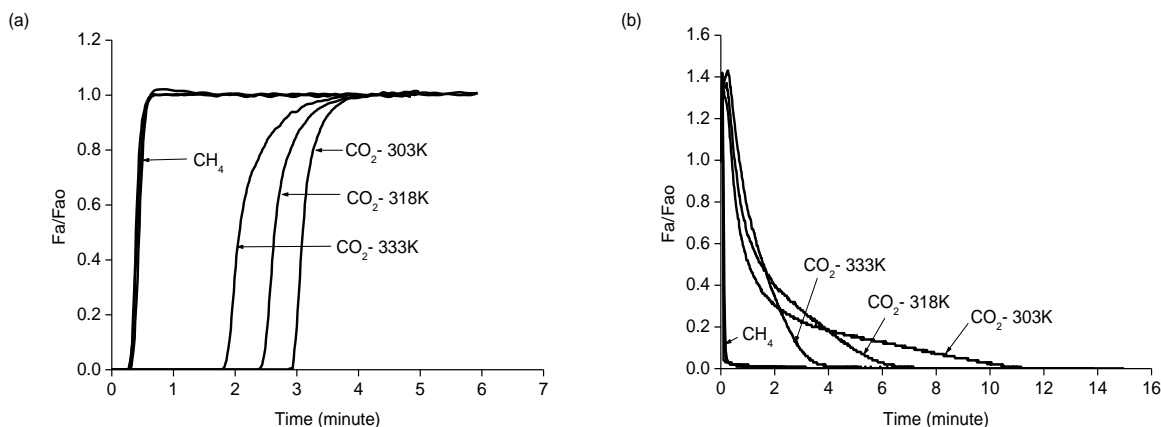


Fig. 4 (a) Adsorption and (b) desorption breakthrough curves of 40% CO₂ - 60% CH₄ in amino-MIL-53(Al) column at 1 bar and different temperatures. (Feed flow rate = 20 Nml/min; desorption by He purging at a flow rate of 20 Nml/min at 1 bar).

4.2 Adsorption-desorption breakthrough curves

The adsorption-desorption breakthrough curves of a 40% CO₂ - 60% CH₄ gas mixture at 303, 318, and 333 K were measured in amino-MIL-53(Al) at a total feed pressure of 1, 5, and 30 bar. Fig. 4 shows the adsorption-desorption breakthrough curves at 1 bar and different temperatures in amino-MIL-53(Al) adsorbent column. CH₄ adsorption breakthrough occurred at almost the same time for all temperatures. No roll-up in the CH₄ curve occurred, which indicates that practically no CH₄ adsorbed in amino-MIL-53(Al). The CO₂ breakthrough time decreased with adsorption temperature and the total amount of CO₂ was similar to the amount adsorbed in the pure component CO₂ isotherm at the particular partial pressure and temperature, as shown in Table 1. The amount of CH₄ adsorbed was practically nil at 1 bar in the

Table 1 Equilibrium adsorption capacities of CO₂ and CH₄ in amino-MIL-53(Al) calculated from pure component adsorption isotherms and adsorption breakthrough curves at different temperatures for a feed composition of 40% CO₂ – 60% CH₄ at a total pressure of 1, 5, and 30 bar.

Gas	Total Pressure (bar)	Partial Pressure (bar)	Amount adsorbed (mmol/g)					
			Isotherm			Breakthrough		
			303K	318K	333K	303K	318K	333K
CO ₂	1	0.4	1.68	1.30	0.90	1.38	1.17	0.92
	5	2.0	2.15	1.92	1.72	2.29	2.07	1.82
	30	12.0	2.86	2.36	2.26	2.87	2.57	2.36
CH ₄	1	0.6	0.04	0.02	0.01	0.01	0.00	0.00
	5	3.0	0.14	0.05	0.04	0.18	0.18	0.17
	30	18.0	1.44	0.41	0.30	2.66	2.00	1.20

breakthrough measurement. The desorption of this saturated amino-MIL-53(Al) column was carried out at isothermal conditions of 303, 318, and 333 K respectively, by purging the column at 1 bar with He at a flow rate of 20 Nml/min. The CH₄ present in the void space of the column eluted very rapidly and also CO₂ desorbed completely with much ease and low dispersion at higher temperature. Fig. 5 shows the adsorption-desorption breakthrough measurements of a 40% CO₂ - 60% CH₄ gas mixture at 5 bar and different isothermal conditions in the amino-MIL-53(Al) column. The amount of CH₄ adsorbed was comparable at all these temperatures, with a value of around 0.18 mmol/g, which was higher than the values obtained from pure component adsorption isotherm of CH₄ in amino-MIL-53(Al) at these temperatures and partial pressure (Table 1). This increase in CH₄ co-adsorption capacity could be due to the transition of amino-MIL-53(Al) framework structure from *vnp* to *np* form in presence CO₂ at this partial pressure [11], which in turn increased the co-adsorption of CH₄ in amino-MIL-53(Al). CH₄ desorbed very rapidly during the dynamic desorption by He purge at 5 bar (Fig. 5b). Desorption of CO₂ was also complete at isothermal conditions, but with a large dispersion at low temperature (303 K). The huge initial peak in the desorption breakthrough curves of CH₄ and CO₂ was due to the sudden release of adsorbed CO₂ and CH₄ by sudden decrease in CO₂ and CH₄ partial pressures when He flow enters the adsorbent column. Fig. 6 shows the dynamic adsorption and desorption breakthrough curves at 30 bar for the same gas mixture in amino-MIL-53(Al). At 30 bar, a significant amount of CH₄ co-adsorbed in amino-MIL-53(Al) as the time lag between the CH₄ and CO₂ breakthrough curves decreased compared to the low-pressure breakthrough curves. The adsorption breakthrough curve of CO₂ at 303 K showed significant dispersion compared to the adsorption breakthrough curves at 318 and 333K. This is attributed to the transition of the framework from *np* form to *lp* form at this high total pressure and the lower isotherm steepness in this form at high pressure (Fig. 2). The dynamic adsorption capacities of CO₂ at 303, 318, and 333 K were almost the same as compared to the pure component isotherm values at the respective CO₂ partial pressure of feed composition (Table 1). However, the amount of co-adsorbed CH₄

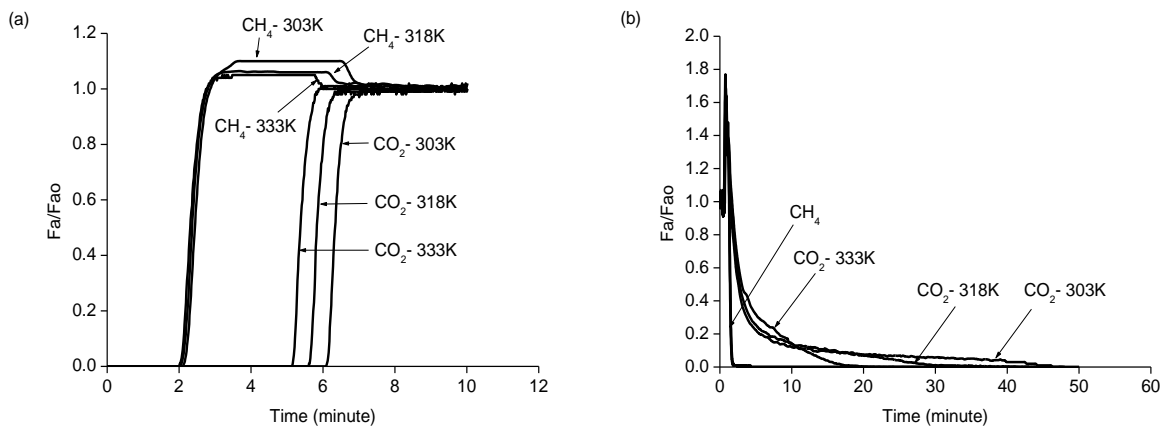


Fig. 5 (a) Adsorption and (b) desorption breakthrough curves of 40% CO₂ - 60% CH₄ in amino-MIL-53(Al) column at 5 bar and different temperatures. (Feed flow rate = 20 Nml/min; desorption by He purging at a flow rate of 20 Nml/min at 5 bar).

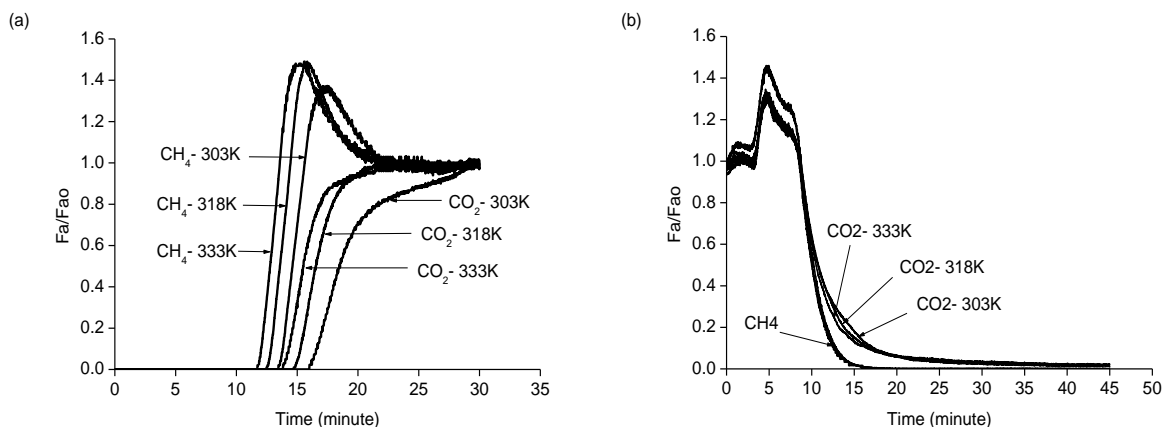


Fig. 6 (a) Adsorption and (b) desorption breakthrough curves of 40% CO₂ - 60% CH₄ in amino-MIL-53(Al) column at 30 bar and different temperatures. (Feed flow rate = 20 Nml/min; desorption by He purging at a flow rate of 20 Nml/min at 30 bar).

was significantly higher in comparison to the pure component adsorption isotherm values at the particular CH₄ partial pressure of the feed composition. This is due to the framework transition at high CO₂ partial pressure in the feed. This co-adsorption mechanism of CH₄ in amino-MIL-53(Al) in presence of CO₂ is schematically represented in Fig. 7. Desorption of CH₄ and CO₂ was carried at 30 bar by purging with He at a flow rate of 20 Nml/min. CH₄ desorbed completely and CO₂ seemed to be desorbed almost completely after about 45 minutes. But in fact, around 82, 74, and 84% of the adsorbed CO₂ only desorbed respectively at 303, 318, and 333K and the remaining amount was trapped inside the adsorbent due to the desorption hysteresis at isothermal conditions. We could release this trapped CO₂ by heating the column.

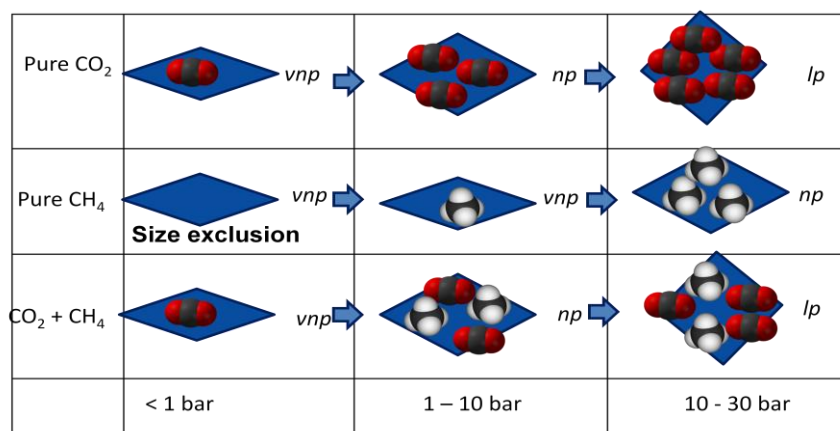


Fig. 7 Schematic representation of CH₄ co-adsorption in presence of CO₂ in amino-MIL-53(Al).

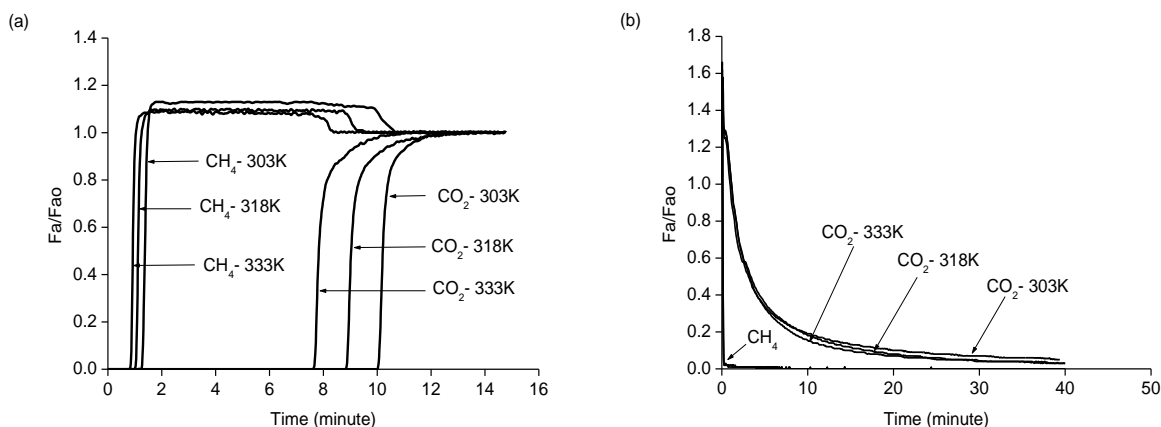


Fig. 8 (a) Adsorption and (b) desorption breakthrough curves of 40% CO_2 - 60% CH_4 in 13X column at 1 bar and different temperatures. (Feed flow rate = 20 Nml/min; desorption by He purging at a flow rate of 20 Nml/min at 1 bar).

For comparison purposes, the adsorption-desorption breakthrough curves of a 40% CO_2 - 60% CH_4 mixture were measured in 13X zeolite, also at a total pressure of 1 and 5 bar. Fig. 8 shows the dynamic adsorption-desorption curves of a CO_2 - CH_4 feed mixture at 1 bar feed pressure and different temperatures. CH_4 eluted first, because of the low adsorption capacity for CH_4 in 13X compared to CO_2 , and showed a roll-up, which was caused by the desorption of pre-adsorbed CH_4 by the advancing CO_2 concentration front along the adsorbent column. CO_2 replaced the adsorbed CH_4 almost completely (Table 2). In desorption, CH_4 from the void space and a little bit adsorbed in the adsorbent eluted rapidly, while desorption of CO_2 was difficult as the CO_2 desorption curve spread out over a very long period (Fig. 8b). By heating the 13X zeolite column, desorption of CO_2 became faster and complete. Fig. 9 shows the adsorption-desorption breakthrough curves of the 40% CO_2 -60% CH_4 gas mixture in 13X

Table 2 Equilibrium adsorption capacities of CO_2 and CH_4 in 13X zeolite calculated from pure component isotherms and adsorption breakthrough curves at different temperatures for a feed composition of 40% CO_2 - 60% CH_4 at a total pressure of 1 and 5bar.

Gas	Total Pressure (bar)	Partial Pressure (bar)	Amount adsorbed (mmol/g)					
			Isotherm			Breakthrough		
			303K	318K	333K	303K	318K	333K
CO_2	1	0.4	4.27	3.52	2.98	4.13	3.55	3.06
	5	2.0	5.35	4.76	4.30	5.26	4.89	4.48
CH_4	1	0.6	0.33	0.26	0.17	0.07	0.07	0.06
	5	3.0	1.35	1.03	0.73	0.12	0.14	0.14

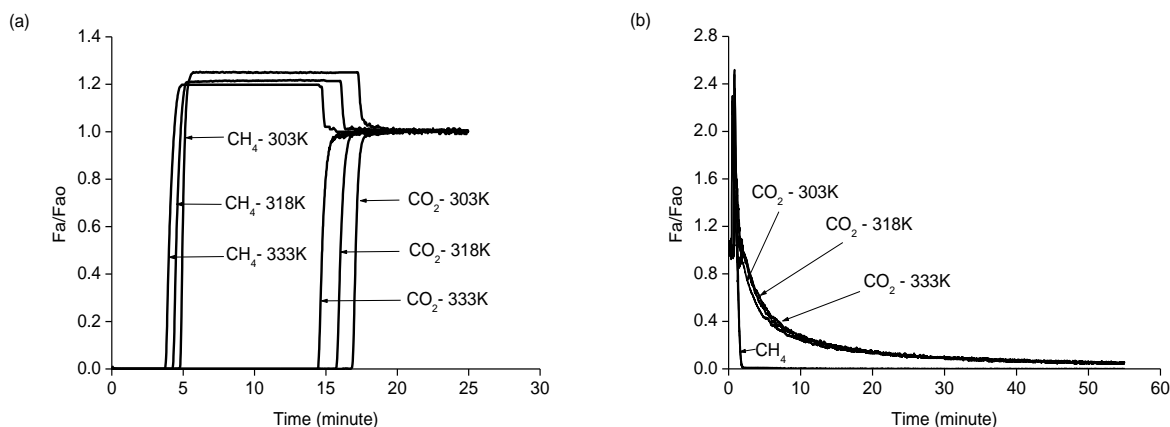


Fig. 9 (a) Adsorption and (b) desorption breakthrough curves of 60% CH₄ and 40% CO₂ in 13X zeolite column at 5 bar and different temperatures. (Feed flow rate 20 Nml/min; He purge flow rate 20 Nml/min at 5 bar).

zeolite at 5 bar. Both CH₄ and CO₂ adsorption breakthrough curves were very steep and CH₄ adsorption breakthrough curves showed very large roll-up. Also at 5 bar, a significant amount of pre-adsorbed CH₄ was replaced by the advancing CO₂ concentration front along the adsorbent column. The net amount of CH₄ adsorbed on 13X zeolite was very low compared to its pure component isotherm adsorption capacities of CH₄ (Table 2). In competitive conditions, strong CO₂ adsorption prevents CH₄ adsorption. In order to remove CO₂ completely from 13 X, high temperatures are needed (Fig. 9b).

Both pure component adsorption (calculated from the pure component isotherms) selectivity as well as dynamic binary adsorption selectivity (from breakthrough measurement) were calculated (Table 3). At 1 bar total pressure, amino-MIL-53(Al) exhibits almost infinite selectivity for CO₂ over CH₄. However, at 5 and 30 bar, amino-MIL-53(Al) displayed lower breakthrough adsorption selectivity than its selectivity based on pure component isotherms, due to high co-adsorption of CH₄ in presence of CO₂. 13X zeolite

Table 3 Both pure component (isotherm) and binary (breakthrough) adsorption selectivities of CO₂ over CH₄ for a feed mixture of 40% CO₂ – 60% CH₄ at different temperatures and a feed pressure of 1, 5, and 30 bar in amino-MIL-53(Al) and, 1 and 5 bar in 13X zeolite.

Adsorbent	Total Pressure (bar)	Selectivity, α_{CO_2/CH_4}					
		Isotherm			Breakthrough		
		303K	318K	333K	303K	318K	333K
Amino-MIL-53(Al)	1	63	98	135	207	∞	∞
	5	23	58	64	19	17	16
	30	3	9	11	2	2	3
13X	1	19	20	26	88	76	76
	5	6	7	9	66	52	48

Table 4 Percentage of CO₂ desorbed at different pressures and temperatures for a period of 3 times the CO₂ breakthrough time in amino-MIL-53(Al) and 13X zeolite.

Adsorbent	Total Pressure (bar)	CO ₂ breakthrough time (minute)			Amount of CO ₂ desorbed at 3 times the breakthrough time (%)		
		303K	303K	318K	303K	303K	318K
Amino-MIL-53(Al)	1	2.9	2.4	1.8	94	100	100
	5	6.1	5.6	5.2	70	85	98
	30	16.0	14.8	13.9	82	74	84
13X	1	10.0	8.8	7.6	65	69	73
	5	16.8	15.7	14.4	55	63	68

showed lower dynamic adsorption selectivity than amino-MIL-53(Al) for CO₂ over CH₄ at 1 bar for all the three temperatures, but at 5 bar its selectivity surmounts that of amino-MIL-53 due to the more efficient displacement of adsorbed CH₄ by CO₂. At 1 bar, amino-MIL-53(Al) showed shape selectivity for CO₂ due to the exclusion of CH₄, as it stay in *vnp* form at low pressure region. In 13X zeolite, the strong electrostatic interaction of CO₂ caused the displacement of weakly adsorbed CH₄, which in turn increased the dynamic adsorption selectivity in 13X. Table 4 shows the dynamic CO₂ desorption efficiency (under isothermal purging with He) in amino-MIL-53(Al) and 13X zeolite in terms of percentage CO₂ desorbed for a period of 3 times the breakthrough time of CO₂ in both these materials. Desorption of CO₂ was very efficient in amino-MIL-53(Al) at isothermal conditions compared to 13X zeolite at both 1 and 5 bar. At 303K, the amount CO₂ desorbed was around 94% in amino-MIL-53(Al) and at higher temperatures, desorption of CO₂ was complete within the particular desorption time. The desorption efficiency was low in 13X zeolite at isothermal conditions due to strong adsorption of CO₂. Only 65 % of the adsorbed of CO₂ could desorb by isothermal purging with He at 303 K and 1 bar. At higher temperatures, the CO₂ desorption efficiency increased in zeolite 13X.

4.3 PSA results

Pressure swing (PSA) and pressure-vacuum swing (PVSA) adsorption were carried out in both amino-MIL-53(Al) and 13X zeolite (Tables 5 and 6). Recovery and productivity increased when the regeneration was carried out under vacuum (PVSA) compared to regeneration by product purging at atmospheric pressure (PSA). In amino-MIL-53(Al), recovery was less compared to 13X zeolite due to its lower capacity for CO₂ compared to 13X zeolite. Cyclic steady state (CSS) was reached very rapidly (< 10 cycles) in amino-MIL-53(Al), whereas in 13X, CSS was only reached after a very long time (> 50 cycles) due to residual CO₂ build up in 13X, which will make the startup procedure of a PSA process using 13X zeolite very complex.

Table 5 PSA results in amino-MIL-53(Al) and 13X zeolite. Cycle steps were feed pressurization (FP), adsorption (AD), blowdown (BD), and purge (PU). Purging at low pressure, $P_L = 1$ bar.

No.	Cycle time(s) FP-AD-BD-PU	P_H (bar)	Feed (Nml/min)	Raffinate (Nml/min)	Purge (Nml/min)	Purity (%)	Recovery (%)	Productivity (molCH ₄ .hr ⁻¹ kg ⁻¹)
Amino-MIL-53(Al)								
1	70 - 80 - 70 - 80	4	20	15.0	5	84.64	36.8	15.4
2	70 - 60 - 70 - 60	4	20	12.8	5	97.64	29.2	12.2
3	70 - 60 - 70 - 60	4	20	12.6	5	99.04	26.0	10.9
4	70 - 50 - 60 - 60	4	20	12.1	5	99.90	21.3	8.9
5	45 - 65 - 45 - 65	3	20	12.6	5	93.96	32.2	13.5
6	45 - 60 - 45 - 60	3	20	12.2	5	95.26	31.4	12.9
7	45 - 50 - 45 - 50	3	20	11.8	5	99.47	29.7	12.4
13X zeolite								
1	90 - 165 - 90 - 165	4	20	13.8	5	97.97	46.4	14.3
2	90 - 145 - 90 - 145	4	20	13.3	5	99.90	40.3	12.4
3	40 - 70 - 40 - 70	4	40	24.5	10	99.95	30.9	19.0
4	40 - 80 - 50 - 70	4	40	29.3	10	91.84	51.9	32.0
5	60 - 145 - 60 - 165	3	20	14.3	5	94.61	51.2	15.8
6	65 - 120 - 65 - 120	3	20	13.3	5	99.95	41.7	12.8

Table 6 PVSA results with amino-MIL-53(Al) and 13X zeolite. Cycle steps were feed pressurization (FP), adsorption (AD), evacuation (EV), and product pressurization (PP). Evacuation at vacuum, $P_L = 0.15$ bar.

No.	Cycle time(s) FP-AD-EV-PP	P_H (bar)	Feed (Nml/min)	Raffinate (Nml/min)	Product Press. (Nml/min)	Purity (%)	Recovery (%)	Productivity (molCH ₄ .hr ⁻¹ kg ⁻¹)
Amino-MIL-53(Al)								
1	70 - 70 - 140 - 0	3	20	15.4	0	92.23	58.7	24.6
2	60 - 60 - 120 - 0	3	20	14.6	0	93.24	56.2	23.5
3	45 - 55 - 110 - 10	3	20	12.6	5	98.54	52.6	22.0
4	45 - 45 - 100 - 10	3	20	12.2	5	99.85	46.2	19.4
5	25 - 55 - 90 - 10	2	20	13.1	5	94.04	65.2	27.3
6	25 - 45 - 80 - 10	2	20	12.4	5	96.73	58.4	24.4
7	25 - 40 - 80 - 15	2	20	12.5	5	98.33	53.3	22.3
8	24 - 36 - 80 - 20	2	20	12.0	5	99.90	45.9	19.2
9	23 - 42 - 80 - 20	2	20	12.0	5	99.60	51.4	21.5
13X zeolite								
1	85 - 165 - 250 - 0	3	20	15.7	0	89.27	76.8	23.7
2	60 - 170 - 250 - 20	3	20	14.6	10	96.39	79.1	24.4
3	80 - 120 - 230 - 30	3	20	13.7	10	99.95	55.8	17.2
4	30 - 180 - 240 - 30	2	20	14.8	10	90.08	84.8	26.1
5	30 - 150 - 210 - 30	2	20	14.4	10	92.56	79.5	24.5
6	30 - 140 - 200 - 30	2	20	14.2	10	93.40	76.4	23.5
7	32 - 128 - 190 - 30	2	20	14.0	10	95.69	74.6	23.0

5 Conclusions

By a combination of isotherm measurements, breakthrough experiments and Pressure Swing Adsorption studies, it was demonstrated that the kinetic separation of CH₄ from CO₂ is possible on amino-MIL-53, at low pressure. Amino-MIL-53(Al) displayed almost infinite dynamic breakthrough adsorption selectivity of CO₂ over CH₄ for a feed mixture of 40% CO₂ – 60% CH₄ at 1 bar pressure. However, the breakthrough selectivity for CO₂ over CH₄ was less than the pure component adsorption isotherm selectivity at 5 and 30 bar due to significant co-adsorption of CH₄ in presence of CO₂ at these pressures. The breakthrough

adsorption selectivity of CO₂ over CH₄ in 13X was higher than the pure component adsorption isotherm selectivity at both 1 and 5 bar. 13X zeolite displayed very high capacity for CO₂, but the desorption of CO₂ was difficult with large spread out in the desorption breakthrough curve, even at 1 bar. CH₄ recovery in amino-MIL-53(Al) was less than that of 13X zeolite due to low CO₂ adsorption capacity in amino-MIL-53(Al) at low pressure. However, using multiple columns and additional cycle steps like pressure equalization, CH₄ recovery could be increased in amino-MIL-53(Al). PSA startup procedure may be easier in amino-MIL-53(Al) due to fast CSS in amino-MIL-53(Al) compared to 13X zeolite. Detailed PSA simulation study is needed for the scale up of the process using amino-MIL-53(Al) adsorbent

References

1. Figueroa, J. D., Fout, T., Plasynski, S., McIlvried, H., Srivastava, R. D.: Advances in CO₂ capture technology—The U.S. Department of Energy’s Carbon Sequestration Program. *International Journal of Greenhouse Gas Control* **2**, 9–20 (2008).
2. Lashof, D. A., Ahuja, D. R.: Relative contributions of greenhouse gas emissions to global warming. *Nature* **344**, 529–531 (1990).
3. Knaebel, K., Reinhold, H.: Landfill gas: From rubbish to resource. *Adsorption* **9**, 87–94 (2003).
4. Cavenati, S., Carlos, A., Rodrigues, A.: Upgrade of methane from landfill gas by pressure swing adsorption. *Energy & Fuels* **19**, 2545–2555 (2005).
5. Delgado, J. A., Uguina, M. A., Sotelo, J. L., Ruiz, B., Rosario, M.: Carbon dioxide/methane separation by adsorption on sepiolite. *Journal of Natural Gas Chemistry* **16**, 235–243 (2007).
6. Ryckebosch, E., Drouillon, M., Vervaeren, H.: Techniques for transformation of biogas to biomethane. *Biomass and Bioenergy* **35**, 1633–1645 (2011).
7. Ruthven, D. M., Farooq, S., Knaebel, K. S.: *Pressure Swing Adsorption*. Wiley-VCH, New York (1994).
8. Ma, S.: Gas adsorption applications of porous metal–organic frameworks. *Pure and Applied Chemistry* **81**, 2235–2251 (2009).
9. Couck, S., Denayer, J. F. M., Baron, G. V., Rémy, T., Gascon, J., Kapteijn, F.: An amine-functionalized MIL-53 metal-organic framework with large separation power for CO₂ and CH₄. *J. Am. Chem. Soc.* **131**, 6326–6327 (2009).
10. Sircar, S.: Separation of methane and carbon dioxide gas mixtures by pressure swing adsorption. *Separation Science and Technology* **23**, 519–529 (1988).
11. Couck, S., Gobechiya, E., Kirschhock, C. E. A., Serra-Crespo, P., Juan-Alcañiz, J., Martinez Joaristi, A., Stavitski, E., Gascon, J., Kapteijn, F., Baron, G. V., Denayer, J. F. M.: Adsorption and separation of light gases on an amino-functionalized metal-organic framework: an adsorption and in situ XRD study. *ChemSusChem* **5**, 740–50 (2012).
12. Pillai, R. S., Peter, S. A., Jasra, R. V.: CO₂ and N₂ adsorption in alkali metal ion exchanged X-faujasite: Grand canonical Monte Carlo simulation and equilibrium adsorption studies. *Microporous and Mesoporous Materials* **162**, 143–151 (2012).

List of Publications

International Journals

1. Sunil A. Peter, Gino V. Baron, Jorge Gascon, Freek Kapteijn, Joeri F. M. Denayer, Dynamic Desorption of CO₂ and CH₄ from amino-MIL-53(Al) Adsorbent. *Adsorption: Journal of the International Adsorption Society* (2013), Accepted.
2. Sunil A. Peter, Gino V. Baron, Jorge Gascon, Freek Kapteijn, Joeri F. M. Denayer, Pressure swing adsorption of CO₂ and CH₄ in amino-MIL-53(Al) for biogas upgradation. (Manuscript under preparation).

Oral Presentation

1. Sunil A. Peter, Gino V. Baron, Joeri F. M. Denayer, Desorption and Pressure Swing Adsorption Studies of CO₂ in Amino-MIL – 53 (Al) for Biogas Upgradation, 11th International Conference on the Fundamentals of Adsorption (FOA11), Baltimore, Maryland, USA, May 19-24, 2013.